JB 90-04

Paper Entitled

"Real-Time Control for a Zero Gravity Robotic End Effector"

Proceedings of

29th CDC Conference

Honolulu, Hawaii
December, 1990

SRC TR 90-13

Proceedings of the 29th Conference
on Decision and Control
Honolulu, Hawaii • December 1990

REAL-TIME CONTROL FOR A ZERO GRAVITY ROBOTIC END EFFECTOR

Carole A. Teolis John S. Baras

Electrical Engineering Department
and Systems Research Center
University of Maryland
College Park, MD 20742

Abstract

The ability to easily manipulate objects in a zero gravity environment will play a key role in future space activities. Emphasis will be placed on robotic manipulation. This will serve to increase astronaut safety and utility in addition to several other benefits. It is the aim of this research to develop control laws for the zero gravity robotic end effector designed by engineers at NASA Goddard. A hybrid force/position controller will be used. Sensory data available to the controller are obtained from an array of strain gauges and a linear potentiometer. Applying well known optimal control theoretic principles, the control which minimizes the transition time between positions is obtained. A robust force control scheme is developed which allows the desired holding force to be achieved smoothly without oscillation. In addition, an algorithm is found to determine contact force and contact location.

1 Introduction

Designing the end effector portion of a *space manipulator*, one must address the problems associated with gripping objects in a zero gravity environment. Reaction forces and torques which are usually damped by various mechanisms (gravity, friction, interaction with the atmosphere) on earth, can create problems in space where these mechanisms are absent. For example, an astronaut attempting to turn a valve on a relatively large space vehicle must be securely attached to the vehicle, otherwise, instead of turning the valve, the torque created will serve to turn the astronaut relative to the vehicle. This is by no means the only difficulty. Consider the following scenario: A master slave arm is being used to link beams for a large space structure. The sockets used to link the beams are transported on trays to the locations of the beam joints. Due to the zero gravity environment, the sockets must be fixed in place by some type of fastener to ensure they remain on the tray. Designing the end effector to release the fastener while maintaining a firm grasp on the socket will solve both the problems associated with torques and reaction forces, as well as the problem of minor perturbations dispersing the sockets in random directions.

Along this line of thinking, NASA has developed the *gripper/nut runner*. This specially designed end effector has two fingers which together have one degree of freedom. Similar to a vice, the width of the opening is the only variable. Centered between the fingers is a device for unscrewing nuts. Having one degree of freedom, the nut runner will be actuated by wrist rotations.

The aim of this research is to develop control laws (in some optimal sense) for the gripper portion of the end effector. A hybrid force/position controller will be used. Sensory data available to the controller are obtained from an array of strain gauges as well as a linear potentiometer. Applying well known optimal control theoretic principles, the control which minimizes the transition time between positions is obtained. A robust force control scheme is developed for smoothly achieving the desired holding force without oscillation. An algorithm is found to determine contact force and contact location in order to ensure a secure grasp.

2 End Effector Model

The finger actuator is a permanent-magnet DC motor. An acme screw serves to transform rotary motion of the motor to linear motion needed to move the fingers. A screw with a small lead angle, $\ell = 1.6\ mm$, is used so that larger finger tip forces can be developed while using a smaller motor. As a trade-off, the maximum velocity attained during opening and closing is lower. Another benefit of having a small lead angle is that the screw is self locking under reasonable load conditions. This is an important feature since it will allow the end effector to hold objects without using power. This property helps to eliminate problems created because of poor heat dissipation in space.

Used to link the motion of the fingers, the rack and pinion gear's effect is to move the fingers at the same velocity in opposite directions. The model, which is developed for the force and velocity of one of the fingers, is effected only by the efficiency, ρ, of this gear.

Deformations of the finger components are assumed to be negligible. This assumption is reasonable since operating forces are far below the magnitude necessary to result in significant deflections of the aluminum body. Because the motion is strictly linear the moving parts in the finger assembly are treated as a point mass. The mass of the moving parts is approximately $1.14\ kg$.

Since the errors due to backlash caused by the gears (the motor's internal gears, the acme screw, and the rack and pinion) will be within desired positioning accuracy of $\pm 0.25cm$, they can be ignored in the model development. Position control will be employed only to achieve an approximate desired finger opening; force control will be used upon encountering an object. Therefore, a coarse positioning scheme will be sufficient.

The system transfer function is given by

$$\begin{pmatrix} F_m(s) \\ V(s) \end{pmatrix} = \frac{1}{d(s)} \begin{pmatrix} \frac{2\pi}{\ell}\mu\rho k_i k_b & \mu\rho k_i M s \\ -\frac{\ell}{2\pi}(L_a s + R_a) & \mu\rho k_i \end{pmatrix} \begin{pmatrix} F_L(s) \\ e_a(s) \end{pmatrix} \quad (1)$$

where $M = (\frac{2\pi}{\ell})^2 J_m + m$ and $d(s) = (\frac{\ell}{2\pi}(L_a s + R_a)Ms + \frac{2\pi}{\ell}\mu\rho k_i k_b)$. The constants and variables are described in tables

constant	definition	value
R_a	armature resistance	25.2 Ω
L_a	armature inductance	7.2 mH
k_i	torque constant	0.4141 Nm/A
k_b	back emf constant	0.6901 $V/rad\ s^{-1}$
J_m	rotor inertia	$2.9 \times 10^{-4}\ kg\ m^2$
ℓ	screw lead	1.6 mm
μ	screw efficiency	0.4
ρ	rack and pinion efficiency	0.7
m	mass of moving parts	1.14 kg

Table 1: *Summary of System Constants*

variable	definition
e_a	control voltage
F_m	finger output force
V	finger velocity
F_L	finger load

Table 2: *Motor Variables*

1 and 2 respectively. For a detailed derivation of the model see [1].

When calculating the position transfer function, $P(s) = sV(s)$, the load force, $F_L(s)$, can be assumed to be identically zero. This is justifiable since position control mode will only be used if there are no external load forces. The position transfer function is

$$\frac{P(s)}{e_a(s)} = \frac{\mu\rho k_i}{s(\frac{\ell}{2\pi}ML_as^2 + \frac{\ell}{2\pi}MR_as + \frac{2\pi}{\ell}\mu\rho k_i k_b)}. \tag{2}$$

The force controller will only be used once a contact force has been detected on one of the fingers. Recall that the target object must be bolted firmly in place in a zero gravity environment. Thus once contact is made, position will become constant forcing the velocity to zero, and the load force, F_L, will equal the motor force, F_m. With these additional constraints the force transfer function is

$$\frac{F_m(s)}{e_a(s)} = \frac{\frac{2\pi}{\ell}\mu\rho k_i}{L_as + R_a}. \tag{3}$$

3 Position Controller

By measuring the gripper's response to a series of sine waves of varying frequencies, the true Bode plot for position may be obtained (figure 1). The accuracy of the true Bode plot for frequency greater than about 3 Hertz is extremely poor due to backlash in the system; this is essentially the *mechanical cutoff frequency* of the system. System performance will not be adversely affected by this low cutoff frequency since the fingers are not intended to make rapid changes in direction.

The actual Bode plot reveals that for the range of operation of the system, only first and possibly second order dynamics are evident. This implies that the third order dynamics caused by the nonzero inductance can be ignored, and thus it can be assumed that the inductance is zero when developing the position controller. Additional friction inherent in the system is apparent in the diminished response of the actual Bode plot.

Substituting $L_a = 0$ into equation 2 gives:

$$\frac{P(s)}{e_a(s)} = \frac{\mu\rho k_i}{s(\frac{\ell}{2\pi}MR_as + \frac{2\pi}{\ell}\mu\rho k_i k_b)} = \frac{c_1}{s(s + c_2)}. \tag{4}$$

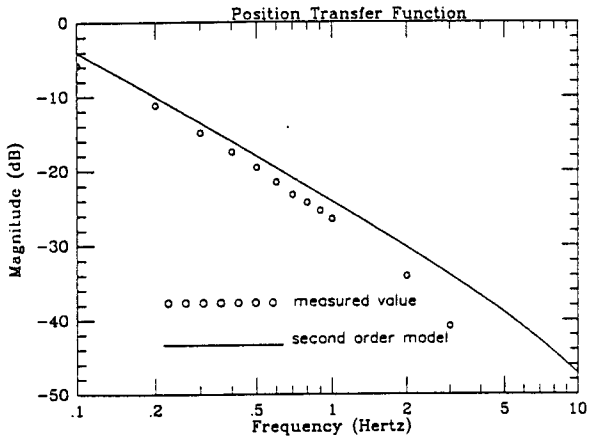

Figure 1: *Theoretical vs. Actual Position Transfer Function*

This transfer function describes a stable linear time invariant system which has one input, the control voltage $e_a(\cdot)$, and one output, the finger position $P(\cdot)$. The minimal realization has two states, finger position $P(\cdot)$, and finger velocity $V(\cdot)$. In state space form, the minimal system is written as

$$\begin{cases} \dot{\mathbf{x}}(t) = \mathbf{A}\mathbf{x}(t) + \mathbf{b}u(t) \\ y(t) = \mathbf{c}\mathbf{x}(t) \end{cases} \tag{5}$$

where

$$\mathbf{A} = \begin{pmatrix} 0 & 1 \\ 0 & -c_2 \end{pmatrix}, \quad \mathbf{b} = \begin{pmatrix} 0 \\ c_1 \end{pmatrix}, \quad \mathbf{c} = \begin{pmatrix} 1 & 0 \end{pmatrix}. \tag{6}$$

Note that since this realization is minimal, it is both controllable and observable. Also, stability of the system guarantees that the eigenvalues of $\mathbf{A}$ have nonpositive real part.

3.1 Optimal Position Controller

It is desirable to determine the control which moves the fingers from the initial state (position, velocity), $\mathbf{x}_0 = (x_0 \quad 0)'$, to the desired final state, $\mathbf{x}_f = (x_f \quad 0)'$, in the minimum time, T^*, with the constraint that $|u(t)| \leq M$. Such problems have been extensively studied in optimization theory. The solution to the minimum time problem follows from the well known Pontryagin Minimum Principle (PMP)[2].

Since the system is linear and controllable, a time optimal control, $u^*(t)$, that transfers the initial state $\mathbf{x}_0$ to $\mathbf{x}_f$ would clearly exist if there were no bounds on the control action. Even with the bounds on the control function, the reachable set at each finite time is convex and bounded and contains the origin. Therefore a time optimal control exists by simple translation of the origin.

Applying PMP it can be shown that the optimal control has the form $u^*(t) = -Msgn(\mathbf{b}'\mathbf{p}^*(t))$, where the costate $\mathbf{p}^*(t)$ satisfies $\dot{\mathbf{p}}^*(t) = -\mathbf{A}'\mathbf{p}^*(t)$.

The Pontryagin Minimum Principle provides both necessary and sufficient conditions for optimality since the system is linear and the constraints convex. Finally the Hamiltonian has a unique global minimum (since it is a minimization of a linear function over a compact convex set). From this and the sufficiency it follows that the optimal control is unique.

3.1.1 Switching Time

The conditions of PMP do not contain any explicit information regarding either the initial costate, $\mathbf{p}^*(0)$, or the terminal

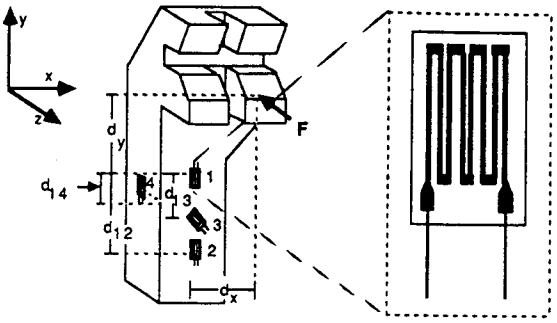

Figure 2: *Strain Gauge Positions*

costate, $\mathbf{p}^*(T^*)$. However, they do imply that the costate, $\mathbf{p}^*(t)$, must be a nonzero vector $\forall t \in [0, T^*]$.

The set of feasible controls, $\mathcal{F}$, is practically limited by the maximum armature voltage, which implies $M = 24V$. And since $\mathbf{b}'\mathbf{p}^*(t) = c_1 p_2(t)$, and $c_1 > 0$, the set of feasible controls is

$$\mathcal{F} = \left\{ u : \; u = \begin{cases} M sgn(p_2(t)) & \text{if } p_2(t) \neq 0 \\ |u| \leq M & \text{if } p_2(t) = 0 \end{cases} \right\}. \quad (7)$$

Another physical constraint is that the control be continuous. Thus if p_2 changes sign the control must vary continuously from M to $-M$. The times at which $p_2 = 0$ are termed the *switching times*. The switching times vary with the initial and final states.

The solution of the costate equation is

$$p_1^*(t) = p_1^*(0) = \text{constant} \quad (8)$$

$$p_2^*(t) = \left(p_2^*(0) - \frac{1}{c_2} p_1^*(0) \right) \exp(c_2) + \frac{1}{c_2} p_1^*(0) \quad (9)$$

Since $p_2^*(\cdot)$ is monotonic in t, the control voltage changes sign at most once.

Notice that the optimal control is directly a function of time, and indirectly a function of position. In order to make the controller robust to disturbances, it is necessary that the dependence on position be made more precise. That is, a more desirable form for the control would be

$$u(x) = \begin{cases} 24 & x_0 \leq x \leq \alpha \\ -24 & \alpha < x \leq x_f \\ 0 & \text{elsewhere} \end{cases} \quad (10)$$

where α is the optimal *switching position* and x_0 and x_f are the initial and final positions respectively.

Using CONSOLE[1], a parametric optimization package, along with SIMNON, a nonlinear simulator, the optimal switching position α was determined. In every case the switching position was found to lie within the allowable position error margins of $\pm .25$ *cm*.

4 Force Controller

Strain data is obtained from an array of four strain gauges on each finger (figure 2). From the strain data, both contact position and force can be calculated. This information will be used to control the holding force as well as to detect an improper grasp.

[1]The implementation details of CONSOLE and SIMNON can be found in [3] and [4] respectively.

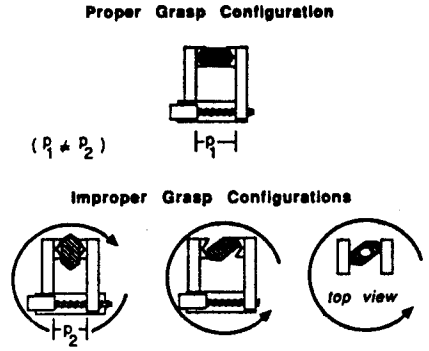

Figure 3: *Grasp Configurations*

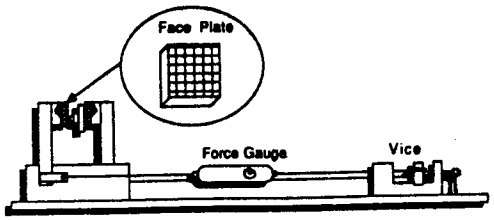

Figure 4: *Experimental Setup for Accurate Force Measurements*

The ability to detect an improper grasp is important since a dropped object may not be easily retrieved. By calculating the contact force and contact locations the security of the grasp as well as the control action needed to correct any errors may be determined. Since the dimensions of the target objects are known, position information may be useful as well. Examples of possible grasp configurations are given in figure 3.

4.1 Determination of Holding Force and Contact Location

It can be shown theoretically that knowledge of the output of eight strain gauges is sufficient to uniquely determine the location and magnitude of the contact force on both fingers[1]. Unfortunately, the accuracy of the derived model may be affected by various disturbances caused by the unmodeled effects of transverse sensitivity, gauge misalignment, zero drift, and temperature dependence. A controller design based on experimentally measured data should be more robust to these disturbances.

An experimental setup for accurately applying forces perpendicular to the face of the gripper finger is depicted in figure 4. With this setup it is possible to empirically measure the sensor output for various holding force magnitudes and positions. Then, from the data, the functional relationship between the strains and the contact force and location can be determined. Note that for this setup forces tangential to the finger face are zero.

The equations which represent the continuous functional relation between the contact force and contact position on each finger, and the strains at the eight gauge locations are nonlinear. The approximation of continuous nonlinear functions is a natural application for neural networks [2]. It has been shown by Cybenko [6], that continuous functions of finite support may be

[2]An in depth discussion of neural networks is beyond the scope of this paper. An excellent introductory reference is the book by Rumelhart and McClelland [5].

approximated by a feed forward neural network with a single (finite) hidden layer. It is thus justified that this topology be used here. Whereas the functional approximation problem could be solved by choosing the form of the solution to be like the model and adjusting the parameters; the neural net solution has the additional advantage that the form of the solution need not be assumed.

The sufficiency proof in Cybenko's paper is nonconstructive and thus does not indicate the required number of neurons in the hidden layer. Using gradient descent (back propagation) to set the weights, the number of neurons is set by trial and error (i.e. If the network can converge to the solution given by the data in the training set, there are enough neurons in the hidden layer.).

For the case where the forces tangential to the finger face are zero, the network solution is found (see section 5).

4.2 Force Controller

Only knowledge of the holding force, F_z, is necessary for force control. Once the desired holding force has been attained at both fingers the contact locations and other force components can be calculated.[1]

Because the surfaces of the gripper fingers are not compliant, attempting to implement a minimum time controller may cause oscillation. Instead an attempt will be made to achieve a smooth response.

The model of the force response is that of an asymptotically stable first order system. Such a system is robust to parameter variation, since the only effect of parameter variation would be to translate the poles of the force transfer function in the open left half plane. A typical controller for a first order system is a simple high gain controller. Theoretically, any finite positive gain could be chosen without destabilizing the system, however, chosing a gain which is *too large* may cause instability due to unmodeled dynamics. In addition, the gain is physically limited by the constraint on maximum armature voltage of $24V$.

The force sensors are the most significant possible cause of feedback destabilization of the force control loop. This is due to the slow response exhibited by the strain gauges when a large force is applied then taken away. Once the force has been removed, the strain gauges may still detect its presence for a very short time. This could easily lead to oscillation. To avoid this a *dead band* can be put in the control algorithm such that if the measured force is *close enough* to the desired force, no control action will be taken.

5 Hardware Implementation

Developing hardware for space applications is a demanding task. In addition to those problems caused by a zero gravity environment, there are a host of others due to the harsh ambient variations associated with earth orbit. Based more on financial than technical reasons, components which do not quite meet specifications were chosen for the prototype. These substitutions should not adversely effect the control methods and algorithms developed here.

Position information is measured using a linear potentiometer. With a minimum theoretical resolution of .025 cm, the errors in position due to the potentiometer fall within the accepted position uncertainty of $\pm.25$ cm.

Using an analog to digital (A/D) converter the potentiometer output voltage is made available to the control algorithm. A linear equation which relates the sensor reading to gripper opening in centimeters was calculated by direct measurements. The constants were chosen to emphasize accuracy in the range of the smaller openings.

Force information is obtained via an array of eight strain gauges. The calculation of the contact force and contact location from the strain data was described in section 4. A Wheatstone bridge is used to measure the small change in resistance of the strain gauge which occurs as the material is strained. A linear approximation of the relation between strain and measured output voltage is made. Again with the aid of an A/D converter the sensor data is made available to the control algorithm.

5.1 Neural Network

Using the experimental setup described in section 4, strain gauge readings were taken for various holding forces and contact locations.[3] The tangential forces are constrained by the experiment design to be zero. In addition, the face plate provides a flat finger face. By imposing these three constraints, the problem is simplified considerably.

The neural network weightings and biases for finger 1 (the long finger) were calculated by the back propagation method.[4] To account for the software requirement that all inputs and outputs of the training data set be normalized to the interval (0,1) define $\tilde{\epsilon_i} \triangleq (\epsilon_i + 20)/300$, where ϵ_i is the output of strain gauge i. The neural network mapping is then described by

$$F_z = \frac{25}{1+\exp(-2.2+19.4\tilde{\epsilon_1}-20.8\tilde{\epsilon_2}-.8\tilde{\epsilon_3})} \quad (11)$$

$$d_y = \frac{8}{1+\exp(-2.2-109.8\tilde{\epsilon_1}+85.5\tilde{\epsilon_2}+2.3\tilde{\epsilon_3})}+1 \quad (12)$$

$$d_x = \frac{8}{1+\exp(1.3+11.7\tilde{\epsilon_1}-22.6\tilde{\epsilon_2}+31.3\tilde{\epsilon_3})}+1. \quad (13)$$

Plots of the actual mapping versus the the neural network mapping are given in figure 5. These results are comparable to those obtained by Naik and Dehoff [7] using a truncated Taylor series approximation.

The apparent error is due not only to errors in the neural net approximation of the nonlinear function, but also to the inaccuracies in the training data. Some of the inaccuracies will be eliminated by the use of higher precision components for the circuit elements such as the Wheatstone bridge and the strain gauges themselves.

5.2 Computer Implementation

The time optimal position controller has been implemented on a Macintosh II equipped with a MacAdios board for D/A and A/D conversions. The controller can position to within $\pm.25$ cm of the desired position without overshoot. The accuracy of the positioning at various openings is reported in figure 6.

Several problems due to strain measurement noise have arisen while implementing the force controller. A significant improvement should be realized by use of higher quality components and wire wrapped circuits. Until the noise problems have been solved, implementation of the contact force and grip point calculation algorithm is virtually impossible. Variations in the strain gauge readings will cause significant errors in the

[3] Data courtesy of Dr. Dipak Naik, Mechanical Engineering Department, University of North Carolina.

[4] The software for this was taken from the Parallel Distributed Processing Software Package by Rumelhart and McClelland.

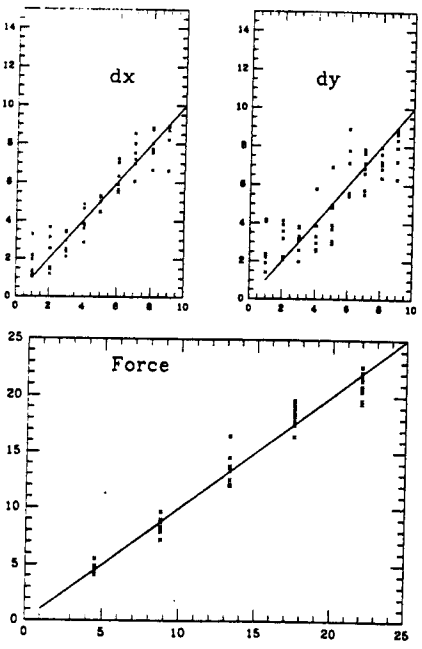

Figure 5: *Actual vs Calculated Values for Holding Force and Position Offset*

calculations since the neural network mapping is based on a certain set of training data. In spite of this the force controller has been implemented but it cannot report an accurate holding force. The operator has the option of choosing one of three levels for the holding force: high, medium, or low. Addressing the problem of hitting an unexpected obstacle, the hybrid force/position controller stops if the prespecified force level is achieved during positioning.

6 Conclusions and Future Research

A position controller has been developed and tested for the gripper portion of the zero gravity robotic end effector. It was determined that an optimal control exists which transfers the initial finger opening to the desired opening in minimum time. This time optimal control is unique and is constant with value equal to plus or minus maximum armature voltage, the value of the control depending on the relative location of the desired final position.

A force controller has been developed and tested which is based only on the holding force, perpendicular to the finger face. In addition, a neural network mapping has been determined to compute contact force and location from the strain data when the tangential force components are constrained to be zero. The percent error between the actual mapping and the neural net mapping is similar to that achieved by the truncated Taylor series used by Naik and Dehoff [7]. It would be interesting to compare the results for a more general case.

Although the successful implementation of the neural network approximation of the mapping from strains to contact force and contact location has not been demonstrated, the approach seems to be a good one. This method offers a simple straight forward approach to this calculation which is unchanged by additional complexity of the mapping.

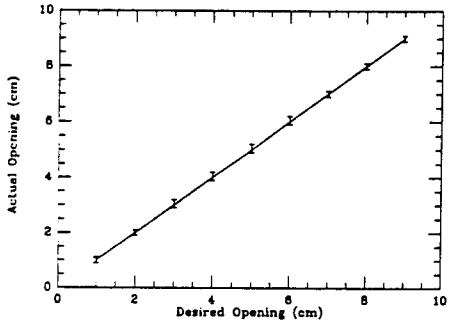

Figure 6: *Positioning Accuracy*

References

[1] C. Salter, "Real-time control for a zero gravity robotic end effector," Masters Thesis, University of Maryland, Department of Electrical Engineering, December 1989.

[2] M. Athans and P. Falb, *OPTIMAL CONTROLS: An Introduction to the Theory and It's Applications.* New York, NY: McGraw-Hill, 1966.

[3] M. Fan, L. Wang, J. Koninckx, and A. Tits, "CONSOLE Users Manual," Tech. Rep. 87-212, Systems Research Center, 1987.

[4] K. Astrom, "A SIMNON tutorial," Tech. Rep., Lund Institute Of Technology, July 1985.

[5] D. Rumelhart and G. McClelland, *Parallel Distributed Processing: Explorations in the Microstructure of Cognition.* Cambridge, Ma.: MIT Press, 1988.

[6] G. Cybenko, "Approximation by superpositions of a sigmoidal function," Technical Report, Tufts University, Department of Computer Science, October 1988.

[7] D. Naik and P. Dehoff, "Design of an Auto Change Mechanism and Intelligent Gripper for the Space Station," Tech. Rep. NAG 5-922, NASA Goddard, 1989.

[8] C. Chen, *Linear Systems Theory and Design.* New York, NY: Holt, Reinhard and Winston, 1984.

[9] Electrocraft Corporation, ed., *DC Motors, Speed Controls, Servo Systems.* Elmsfor, NY: Pergamon Press, fifth ed., 1980.

[10] A. Window and G. Holister, eds., *Strain Gauge Technology.* Essex, England: Applied Science Publishers, 1982.